Investigation of the Mechanical and Wear Properties of Epoxy Resin Composite (ERCs) Made With Nano Particle TiO2 and Cotton Fiber Reinforcement

Naveen Kumar Yadav
Department of Mechanical Engineering, Amity University Rajasthan

Nitesh Singh Rajput
Department of Mechanical Engineering, Amity University Rajasthan

kulshreshtha, Shweta
Amity Institute of Biotechnology, Amity University Rajasthan

Manoj Kumar Gupta
Department of Mechanical Engineering, Hemvati Nandan Bahuguna Garhwal University

https://doi.org/10.5109/6781041

出版情報：Evergreen. 10 (1), pp.63-77, 2023-03. 九州大学グリーンテクノロジー研究教育センター
バージョン：

Investigation of the Mechanical and Wear Properties of Epoxy Resin Composite (ERCs) Made With Nano Particle TiO2 and Cotton Fiber Reinforcement

Naveen Kumar Yadav[1], Nitesh Singh Rajput[1*], Shweta kulshreshtha[2], Manoj Kumar Gupta[3]

[1]Department of Mechanical Engineering, Amity University Rajasthan, India - 303002

[2]Amity Institute of Biotechnology, Amity University Rajasthan, India- 303002

[3]Department of Mechanical Engineering, H.N.B. Garhwal University, India- 246174

*Author to whom correspondence should be addressed:
E-mail: nsrajput@jpr.amity.edu

(Received December 8, 2022; Revised February 5, 2023; accepted March 19, 2023).

Abstract: Epoxy composites reinforced with cotton fibers and incorporating TiO2 nanoparticles were studied at room temperature. The mechanical behavior of 0.5% to 2% TiO2 hybrid composites with cotton fiber fabric, ranging from single to multi-layer, was examined. The Taguchi method was used to improve the mechanical and wear attributes of the hybrid composites. The experiments were conducted using an L16 array, and mechanical tests were performed using an L16 orthogonal array to evaluate the impact of TiO_2 (0.5%, 1%, 1.5%, 2%), cotton fiber fabric (1, 2, 3, 4 layers), and epoxy resin. Load in kilograms (1, 1.5, 2, 2.5) and speed in RPM (200, 250, 300, 350) were specified as control parameters for the wear testing of ERCs. The wear test rotation distance was 200 meters.

The addition of nanoparticles to ERCs reinforced with cotton fibers significantly decreased the wear rate, with hybrid composites containing 2% TiO_2 nanoparticles exhibiting the lowest wear rate. Increasing the percentage of nanoparticles and cotton fiber reinforcement improved the mechanical strength of the ERCs. According to the results of the ANOVA analysis, load was the factor that most significantly influenced the wear rate, followed by speed and finally the weight percentage of nanoparticles. The ANOVA results clearly showed that TiO_2 nanoparticles had the largest influence on the wear rate, with a contribution of 65.43%. The second most significant factor was the rotation of the disk, with a contribution of 23.91%. Although cotton fiber fabric had the least significant impact on the wear rate, the load factor still contributed 4.34% to the total.

Keywords: Hybrid composite, nano particle, cotton cloth reinforcement, Taguchi method, ANN, machine learning, TiO_2

1. Introduction

Epoxy resin composites, also known as ERCs, are widely used in various industries such as automotive, sports and recreation, aviation, marine, civil, biomedical, and others. This is due to the improvement of the matrix properties through reinforcement, making ERCs suitable for a diverse range of applications. The reinforcement materials blended into the epoxy resin matrix result in improved tribological and mechanical properties compared to the original matrix. The strengthened structure allows for these improved qualities, making ERCs a valuable material for various applications. [01-05)].

Natural fiber reinforced composites attract researchers due to their characteristics such as biodegradability, low environmental impact compared to pure plastic, availability, light weight, cost-effectiveness, toughness, and suitability for various applications. However, limitations such as weak fiber-matrix bonding and significant moisture absorption hinder their use. Some natural fibers, like Jute, Sisal, Flax, and Hemp, need to be processed before use. Jute fibers have properties that meet the high strength-to-weight ratio requirements for composites.[6-8, 66, 67)].

By filling epoxy with a variety of fillers and then curing the mixture, the composites combine the superior chemical and physical properties of both the epoxy and fillers. The introduction of a silk fiber reinforcing mat in poly-e-caprolactone, which is a biodegradable polymer, resulted in a 45 percent and 35 percent enhancement in the bending and tensile strengths of the polymer, respectively[9)]. The flexural and Young's modules of a polylactic acid composite reinforced with short silk fibers were increased by 5% and 25%, respectively[10)].

In industrial sectors, such as agriculture, mining, mineral processing, and earth movement, abrasion has a significant impact when handling dirt, rock, or minerals. The three-body abrasive wear process allows the grits to freely roll and slide on the surface, making them more effective. The field of tribology aims to understand wear, friction, and lubrication that occur between moving surfaces in relative motion. According to an analysis, abrasion is responsible for 80-90% of the overall wear of machine elements, while fatigue accounts for the remaining 8%.[23)]

The purpose of this study was to investigate the mechanical behavior and wear attributes of epoxy composites reinforced with cotton fiber and incorporating TiO_2 nanoparticles at room temperature. The experiment used Taguchi methodology and an L16 array to test the impact of various factors such as TiO_2 (0.5-2%) content, number of layers of cotton fiber fabric, load and speed on the wear rate of the composites. The results showed that the addition of TiO_2 nanoparticles and cotton fiber reinforcement improved the mechanical strength and decreased the wear rate of the composites. The analysis of variance revealed that the most significant factor affecting the wear rate was the content of TiO_2 nanoparticles, followed by the rotation distance and then the load. The study concluded that the TiO_2 nanoparticles had the largest impact on the wear rate of the composites, contributing 65.43% to the total.

2. Literature Review

Prasob et al.[11)] investigated the mechanical properties and dynamic characteristics of ZnO- and TiO_2-filled woven jute/epoxy composites at temperatures of 40, 20, and 27°C. In this work, the mechanical strength of jute fiber and epoxy composites was discussed for both fiber and filler boundary conditions. The results showed that the mechanical properties and dynamic behavior of woven jute/epoxy composites filled with ZnO and TiO_2 were superior to those of unfilled TiO_2. The tensile and compressive properties of the composite containing TiO_2 were significantly improved.

The authors (K. Kumar et al)[12)] conducted an investigation to study the effect of changing the weight percentage of TiO_2 nanoparticles in epoxy from 5%, 10%, to 15% on the mechanical properties and dynamic physical behavior of a matrix formed through high-frequency twin mixing. The composite was created through ultrasonic dual mixing, where simultaneous mixing was performed using a stirrer and the dispersion of TiO_2 was observed using a field emission scanning electron microscope (FE-SEM).

The author (Suresha et al)[7)] of the article conducted research on the mechanical and corrosive wear properties of jute fabric reinforced polymer with varying weight percentages of micro-sized TiO_2. The results showed that mechanical properties can be enhanced with the addition of TiO2 particles up to 7.5% weight fraction, and the abrasion resistance of the composite was observed to increase with a weight fraction of up to 5% TiO_2. These findings align with the hypotheses.

Epoxy composites that have functionally graded components and are reinforced with titanium dioxide (TiO_2) have been the focus of the Siddhartha et al research work[8)] When compared to homogenous composites, the addition of TiO_2 particles to epoxy had a substantial influence on the material's flexural strength, tensile modulus, and interlaminar strength. This was true despite the fact that the homogenous composites had varying degrees of strength.

Alshammari et al[13)] studied the tribological performance of jute-epoxy based composites in different jute mat orientations. The results of the research revealed that fiber orientation had a significant impact on the wear and friction performance. The author concluded that the wear rigidity was better in the trigonal orientation and that jute fiber showed promise as a replacement for synthetic materials such as glass under similar operating conditions. The study utilized a scanning electron microscope to examine the effect of base shear on the fiber-matrix interface at various orientations and applied shear force to the fiber-matrix interface in each orientation.

The Bhargav et al[14)] conducted research to investigate the mechanical characteristics and erosion wear behavior of jute fiber reinforced composites with varying fiber orientations and the addition of titanium dioxide. The composite samples were created using woven jute fiber as a filler material at a weight percentage of 2%. The fibers were arranged in various directions. The results showed that the tensile and flexural properties of the jute fiber/epoxy composite improved with the addition of TiO_2 filler material, and the erosive wear resistance improved at a fiber orientation of 90 degrees. However, the orientation of the fiber did not have a significant impact on the erosive wear rate.

Due to their extremely small size, micron-sized particles are attracted to each other by van der Waals forces, forming agglomerates. Studies have shown that incorporating these particles into a material can significantly improve its mechanical properties, such as raising the modulus of filler-filled epoxy. Inspired by these findings, we explored the potential of incorporating micron-sized TiO_2 particles into jute fabric-reinforced epoxy composite materials. Our goal was to examine how these particles would impact the mechanical properties and abrasive wear resistance of the composites[15-18)].

The mechanical properties of silicon dioxide filled glass/epoxy composites have been investigated by the Osmani et al[19)], who reported that the flexural strength and modulus increased with an increase in the filler loading, while the tensile and shear strengths decreased with an increase in the silicon dioxide content.

The Alavudeen et al[20)] of the study investigated the mechanical properties of composites made from woven banana fiber, kenaf fiber, and a hybrid of the two. The

hybridization process resulted in improved tensile, flexural, and impact strengths of the woven composites. These improvements were attributed to the presence of both kenaf and banana fibers in the hybrid structure.

Swain et al. [21] conducted a study on the physico-mechanical properties of jute fiber reinforced epoxy hybrid composites filled with alumina. The combination of jute and alumina as hybrid reinforcements in epoxy was found to result in improved characteristics as the fiber and filler loading increased. This was evidenced by increased hardness, strength, flexural modulus, and tensile modulus when more fiber and filler was added. The researchers concluded that the material's properties improved with increased fiber and filler loading.

Mantry et al.[22] conducted a study on the tensile properties of jute/epoxy hybrid composites, both unfilled and filled with SiC particles. The researchers found that an increase in fiber loading in the composite material led to a rise in tensile strength for the unfilled jute/epoxy material. However, the strength of the SiC-filled jute/epoxy composites decreased when the SiC loading was increased, contrary to expectations.

In applications that need abrasion resistance, natural fibers such as coir, coconut coir sheath, bamboo, sugar cane, waste silk, oil palm, ipomoea carnea, and banana have been found to be excellent and effective reinforcement in thermoset matrices[24-27]. According to various researchers, natural fibers must undergo a chemical treatment to make them compatible with thermoset polymers, leading to improved mechanical properties of the composites. Surprisingly, there is limited research in the tribology literature exploring the tribological behavior of natural fibers in reinforced polymers. Additionally, the number of studies examining the abrasive wear behavior of woven natural fibers without fillers is also quite low.[28-32, 57-59].

Epoxy is one of the most often employed matrix materials in the composites manufacturing process. It may be obtained at room temperature for low expense and minimal effort in the form of resin. Epoxy's ability to make a strong bond with fibers has led to its widespread usage in reinforcing natural fibers, according to published studies[33]. Because of how rapidly it cools, it may be utilized to create a variety of composite products. It retains sufficient strength and may be altered to function as a composite with a high load bearing capacity[34, 65, 66].

Karthik et al[60] analyzed the effect of incorporating 2% nano titanium oxide and 5% polyaramid fibers into an epoxy matrix composite strengthened with jute, bagasse, and coir fibers on the composite's structure and properties. Biocomposites were manufactured using the hand lay-up method with a 40% fiber and polyaramid composition. Thermal stability was analyzed using TGA experiments, revealing a 5-step thermal degradation process with the slowest step (the 2nd step) determining the rate. Broido plots indicated the first step of heat degradation had the lowest activation energy due to the reduced energy needed to remove hemicellulose and water in the bagasse fiber.

The purpose of this study is to investigate the effect of combining carbon, glass, and Kevlar bidirectional (0°/90°) woven mat synthetic fibers reinforced in an epoxy matrix composite with silicon carbide (SiC) nanoparticles as filler material on the mechanical and visco-elastic properties of newly developed hybrid polymer matrix composites (HPMCs). Six different sequences of stacking six layers of carbon, glass, and Kevlar fibers were utilized in the production of the composites through vacuum bag infusion method. Testing, in accordance with ASTM standards, was done to determine the composite with the best mechanical characteristics, including tensile, flexural, impact, and hardness tests.[61, 62, 63, 64]

The primary objective of the current experiment was to investigate the impact of cotton fiber fabric (CFF) and TiO_2 Nanoparticle on the physio-mechanical properties and wear characteristics of epoxy. The CFF was treated with NaOH solvent, and the effect of the treatment was evaluated as part of this study. The Taguchi approach of experimental design was utilized to create an experiment table with four parameters and four levels. The focus of this work was on the tensile strength and wear rate of the composite material, which were then optimized using advanced methods.

2. Materials and Methods

2.1 Materials Selection

Epoxy Resin (LY-556)[35, 36, 37] was chosen as the matrix material for this study due to its superior mechanical, thermal, and anti-corrosive properties. To initiate the chemical reactions, the epoxy resin and hardener (HY-951) had to be mixed together. The properties of the epoxy resin purchased from a local dealer in Jaipur, Rajasthan, India are listed in Table 1. The composite material was produced using a 10:1 ratio of epoxy resin and hardener (10:1)[40]. To improve the tribological and mechanical properties of the composite, reinforcing components such as TiO_2 nanoparticles and NaOH-treated cotton fiber fabric (CFF) were used[38]. According to the particle distribution measurements, the average particle size of TiO_2 nanoparticles was between 50 and 100 mm, as shown in Figure 1.

The novelty of this research lies in the utilization of the hand lay approach in the development of epoxy resin composites incorporating TiO_2 nanoparticles and CFF layers. The research aimed to investigate the impact of these components on the properties of the composite, specifically the wear rate. The use of the hand lay approach, while challenging during fabrication, allowed for the creation of the composite and the experiment table was constructed using the Taguchi approach. The results of the ANOVA table showed the weight percentage of TiO_2 having the largest influence on the composite's wear rate, a finding that highlights the significance of this component in the development of ERC composites.

Furthermore, the research also investigated the impact of the weight percentage of CFF and TiO_2 on the composite's water absorption capacity and void fraction. In summary, the novelty of this research lies in its contribution to the field of ERC composites by investigating the impact of the hand lay approach and the incorporation of TiO_2 nanoparticles and CFF layers on the properties of the composite. The findings have the potential to lead to further advancements in the field and provide useful information for future research.

Table 1 Properties of the Epoxy Resin (LY-556) and Hardener (HY-951) [14, 40)]

Physical Property	Specifications	LY-556	HY-951	Unit
Density	ISO 1675	1.15-1.20	0.97-0.99	gm/cc
Viscosity	ISO 12058	10k-12k	10-20	mPa.s
Flash Point	ISO 2719	>200	>180	C
Ultimate Tensile Strength	-	82	50	MPa
Color	-	Clear Transparent	Clear Transparent	-

Table 2 presents the material specifications that were utilized for the composite fabrication, Included in this table is a listing of all of the components.

Table 2 Materials Specification required for fabrication of Composite

Constituents	Specifications
Epoxy	LY-556
Hardener	HY-951
Nano Particle (As Filler)	TiO_2 (Approx 50-100 nm)
Reinforcement	Cotton fiber fabric (CFF) Approx 120 GSM

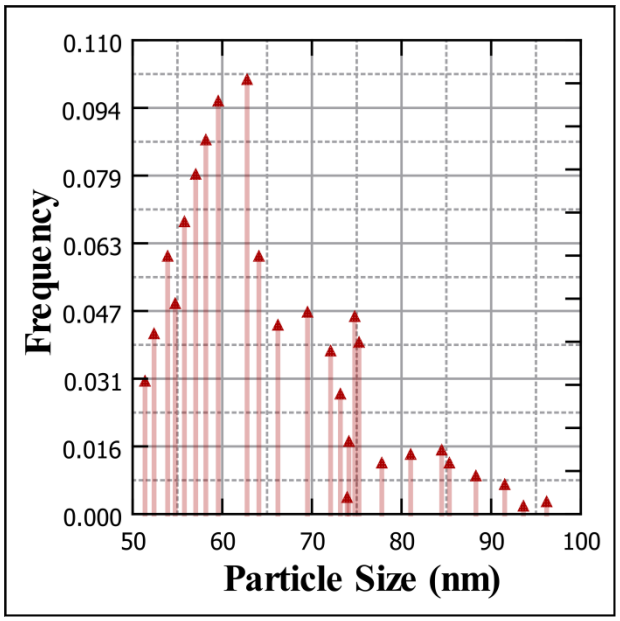

Figure 1 TiO2 TEM image for particle distribution and Histogram

The average gap among CFF was shown in figure 2 using digital microscope. The average gap among CFF is measure using image processing software image**J[41)]** was found in range of 0.5 mm to 2 mm. The real and binary image was shown in figure 2.

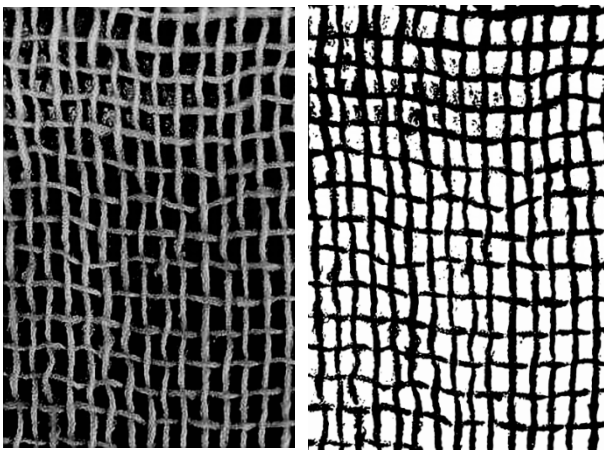

Figure 2 CFF gap measurement using image processing technique[41)] a. (Original image) b. (Binary Image)

2.2 Chemical Treatment of CFF

During the preparation of a 5% by weight NaOH solution, 5 grams of NaOH powder were mixed with 100 grams of water[38)]. The CFF was kept in the solution for over 24 hours before being removed. After being extracted from the solution, the fibers were rinsed with deionized water. To eliminate any residual moisture, the purified CFF fibers were dried under direct sunlight. The figure 3 illustrates the sodium hydroxide treatment of the CFF fibers (NaOH).

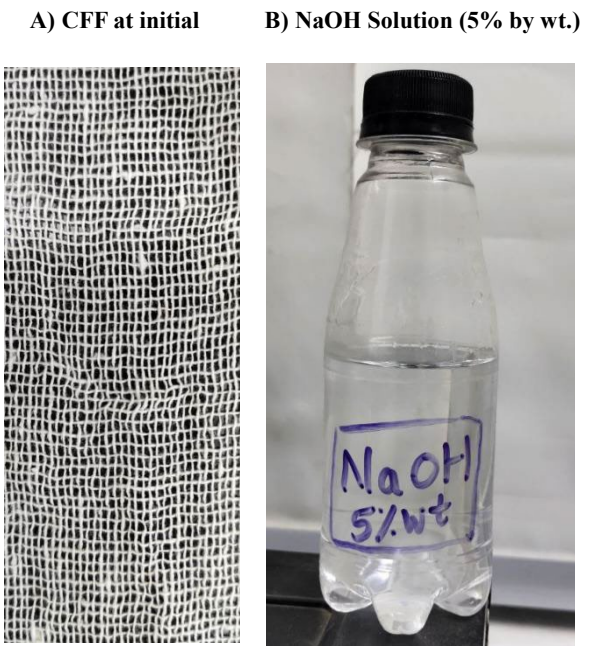

Figure 3 Chemical treatment of CFF using NaOH solution[38)]

2.3 Compositions for Fabrication of Composite

In this study, the composite was produced using design of experiment (DOE) procedures. The selection of components and their quantities were made in accordance with DOE guidelines. The results of the investigation are summarized in Table 3, including the final factor and level selections made for the study.

Table 3 Factors and Levels

Coded Name	Controlling Parameters	L-I	L-II	L-III	L-IV
A	**TiO_2 (wt%)**	0.5	1.0	1.5	2.0
B	**CFF (layers)**	1	2	3	4
C	**Load (kg)**	1.0	1.5	2.0	2.5
D	**Speed (RPM)**	200	250	300	350

In this study, mechanical and wear analysis were crucial, as shown in Table 3. Factors A and B were needed for fabricating the composite, while factors C and D were required to evaluate the wear properties of the composite formed using epoxy resin as the matrix material. The total weight of the composite was kept constant at 100 gm without including the CFF weight at the initial levels.

2.4 Fabrication

The first step in the fabrication process was to combine epoxy (LY-556) and hardener (HY-951) at a ratio of 10:1, then magnetic stir the mixture for fifteen minutes[1)]. The CFF was arranged in layers that were making straight after being pressed. The fabrication of the composite was accomplished by the use of the hand lay up method[42)]. Rectangular molds made of silicon rubber can be purchased from local vendors. After the epoxy and hardener mixture was prepared, it was poured into the mold and the CFF layers were arranged according to the experimental table. The mold was then left to cure at room temperature for over 24 hours. Two separate samples were made for each mixture that was tested. After one day, the samples were finally removed from the mold and test specimens were prepared according to ASTM standards.[43, 44, 45, 46)].

Table 4 Total weight of the components required for composite for fabrication

Run Order	TiO_2 (gm)	Epoxy (gm)	Total (gm)	CFF (gm)
1	0.5	99.5	100	2.2
2	0.5	99.5	100	5.1
3	0.5	99.5	100	6.3
4	0.5	99.5	100	8.2
5	1	99	100	2.2
6	1	99	100	5.1
7	1	99	100	6.3
8	1	99	100	8.2
9	1.5	98.5	100	2.2
10	1.5	98.5	100	5.1

Run Order	TiO_2 (gm)	Epoxy (gm)	Total (gm)	CFF (gm)
11	1.5	98.5	100	6.3
12	1.5	98.5	100	8.2
13	2	98	100	2.2
14	2	98	100	5.1
15	**2**	98	100	6.3
16	**2**	98	100	8.2

During fabrication, the overall weight was kept at its baseline of 100 gm, excluding the weight of the FCC fabric. The overall weight, calculated using the weights of TiO_2, CFF, and epoxy resin (as a balance weight), is displayed in Table 4. This table was used in the fabrication process of the composite materials for this experiment. The component weights were measured using a digital weighing machine.

3. Design of Experiment

The Taguchi method was used to create the experimental matrix. The analysis focused on the impact of the input factors on the mechanical and wear behavior of the composites. Table 3 lists the various influencing elements and their levels. For this investigation, four levels were selected for each variable. The experiment design employed the L-16 orthogonal array along with the MINITAB-18 statistical program.[47], as displayed in Table 3. The signal-to-noise ratio, or SNR (eq.1.1)[48], is evaluated using the Taguchi technique by calculating the degree to which an attribute deviates from its selected values. The results of the experiment were expressed as a ratio of signal to noise. Due to the fact that the mechanical wear study was conducted on TiO_2 and CFF-reinforced composites, the smaller-is-better quality measure was taken into consideration throughout this investigation. The final DOE L-16 experiment table was shown in table 5.

$$S/_N = -10\log\frac{1}{n}\left(\sum_{i=1}^{n} y_i^2\right) \quad (1)$$

Where S/N represents the ration of the signal to ratio of the response parameters, n is the experiment repetition for more accurate results, y represents the response data for each experiment run (i).

Table 5 Experiment design by taguchi method using L-16 orthogonal array

Run Order	A TiO_2 (%wt)	B (layers of CFF)	C Load (kg)	D Speed (RPM)
1	0.5	1	1	200
2	0.5	2	1.5	250
3	0.5	3	2	300
4	0.5	4	2.5	350
5	1	1	1.5	300
6	1	2	1	350
7	1	3	2.5	200
8	1	4	2	250
9	1.5	1	2	350
10	1.5	2	2.5	300
11	1.5	3	1	250
12	1.5	4	1.5	200
13	2	1	2.5	250
14	**2**	2	2	200
15	**2**	3	1.5	350
16	**2**	4	1	300

4. Result and Discussion

4.1 Density Analysis

Density and void fraction are estimated using equations 2 and 3 in this section. The density of matrix material was supposed to be 1.25 g/cm3[39], while the density of CFF was considered to be 1.14 g/cm3[49,50] and the density of nanoparticles (TiO_2) was assumed to be 4.175 g/cm3[51]. All of these numbers are utilized to calculate the composite's theoretical density according to DOE table L-16. After calculating the theoretical density, the experiment density was measured before calculating the void fraction.

$$\rho_{th} = \frac{1}{\frac{Wt_{er}}{\rho_{er}} + \frac{Wt_{np}}{\rho_{np}} + \frac{Wt_{CFF}}{\rho_{CFF}}} \quad (2)$$

Here Wt represents the weight percentage, ρ represents the density. The Wt was list out in table 6 for calculation of theoretical density of the composite material. Experimental density was measured two times and then average value was recorded into the table 6.

$$V_f = \frac{\rho_{th} - \rho_{exp}}{\rho_{th}} \quad (2)$$

The theoretical and experimental densities of CFF and TiO2-epoxy composites are presented in Table 6. The presence of voids in the material, resulting from the manufacturing and curing processes, is the reason for the lower experimental densities compared to the theoretical densities of all compositions. The formation of voids is due to the non-homogeneous distribution of CFF within the epoxy matrix[1]. Increasing the nanoparticle content of

the matrix material was observed to help manipulate these non-homogeneous properties, as seen in Figure 4, but it also revealed that these non-homogeneous properties could be controlled by adding nanoparticles to the matrix material.

Table 6 Void Fraction and Density of Composite

Run Order	TiO_2 (%wt)	CFF (%wt)	ER (%wt)	Total (% Wt)	Density-Th	Density-Exp	Void Fraction
1	0.50	2.15	97.36	100	1.252	1.228	1.89
2	0.50	4.85	94.67	100	1.248	1.208	3.23
3	0.50	5.93	93.60	100	1.247	1.184	5.05
4	0.50	7.58	91.96	100	1.245	1.167	6.26
5	1.00	2.15	96.87	100	1.256	1.243	1.04
6	1.00	4.85	94.20	100	1.252	1.231	1.72
7	1.00	5.93	93.13	100	1.251	1.212	3.12
8	1.00	7.58	91.50	100	1.249	1.201	3.84
9	1.50	2.15	96.38	100	1.260	1.241	1.53
10	1.50	4.85	93.72	100	1.257	1.238	1.49
11	1.50	5.93	92.66	100	1.255	1.231	1.93
12	1.50	7.58	91.04	100	1.253	1.224	2.31
13	2.00	2.15	95.89	100	1.265	1.258	0.53
14	2.00	4.85	93.24	100	1.261	1.247	1.10
15	2.00	5.93	92.19	100	1.259	1.242	1.38
16	2.00	7.58	90.57	100	1.257	1.237	1.60

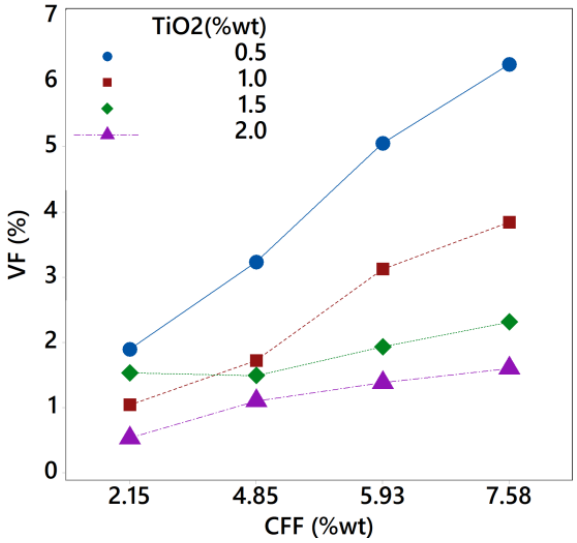

Figure 4 (a) Void Fraction of Composite material (CFF and TiO2)

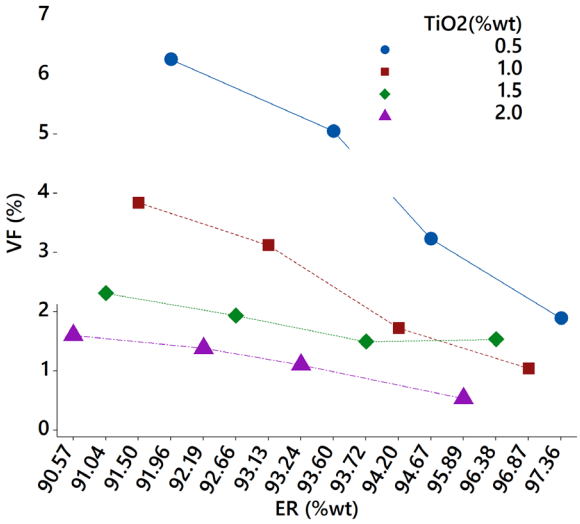

Figure 4 (b) Void Fraction of Composite material (ER and TiO2)

Figure 4a depicts that as the weight percentage of CFF in the composite material increases, the void fraction also increases. However, the void fraction can be controlled by increasing the weight percentage of nano particle TiO2, as shown in Figure 4b. On the other hand, when the weight percentage of epoxy resin in the matrix component increases relative to the nano particle, the void fraction

decreases. Figure 4c illustrates that an increase in the weight percentage of CFF in the epoxy resin results in an increase in the void fraction.

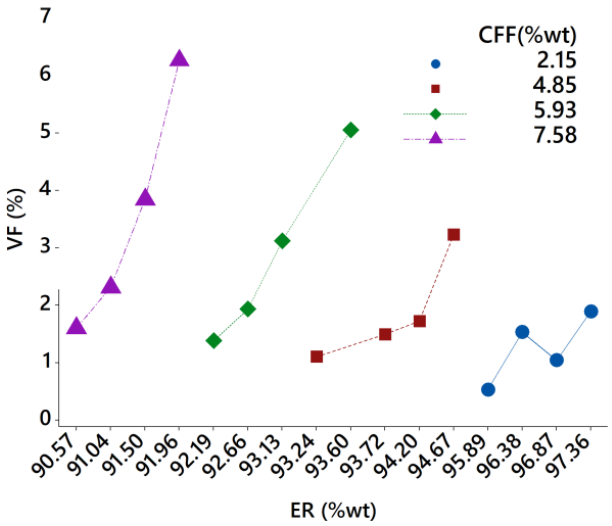

Figure 4 (c) Void Fraction of Composite material (ER and CFF)

4.2 Water Absorption Analysis

The water intake of the sample was measured by submerging it in distilled water in a controlled environment for 20 days[1)], or until the composite was completely saturated, whichever came first. The following equation was used to make an estimate of the water absorption rate for the sample both before and after it was immersed in water. Daily weight readings were taken both before and after the immersion. The water absorption (WA) analysis for L-16 was list out in table 7. The plots for water absorption was shown in figure 5.

$$WA_{in\,\%} = \frac{(Wt_{ini} - Wt_{fn})}{Wt_{ini}} \qquad (3)$$

Table 7 Water Absorption analysis for L-16 orthogonal array

Run Order	TiO_2 (gm)	CFF (gm)	ER (gm)	Initial Wt (gm)	Final Wt (gm)	WA (%)
1	0.5	2.2	99.5	102.2	103.9	1.68
2	0.5	5.1	99.5	105.1	106.9	1.72
3	0.5	6.3	99.5	106.3	109.2	2.74
4	0.5	8.2	99.5	108.2	111.0	2.59
5	1	2.2	99	102.2	103.1	0.85
6	1	5.1	99	105.1	106.7	1.50
7	1	6.3	99	106.3	108.3	1.88
8	1	8.2	99	108.2	110.7	2.31
9	1.5	2.2	98.5	102.2	103.2	0.99
10	1.5	5.1	98.5	105.1	106.0	0.86
11	1.5	6.3	98.5	106.3	107.6	1.20
12	1.5	8.2	98.5	108.2	109.8	1.45
13	2	2.2	98	102.2	102.5	0.32
14	2	5.1	98	105.1	105.8	0.69
15	2	6.3	98	106.3	107.2	0.87
16	2	8.2	98	108.2	109.2	0.96

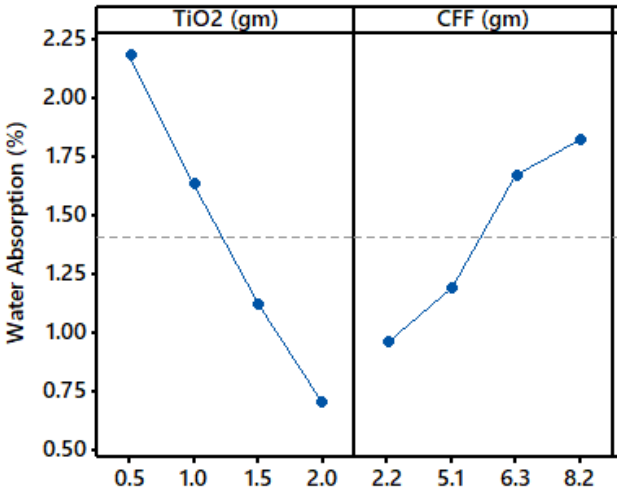

Figure 5 Water Absorption analysis for L-16 orthogonal array

As shown in Figure 5, the addition of CFF to epoxy resulted in a significant increase in the material's water absorption capacity. This was expected as epoxy is hydrophobic, while CFF is hydrophilic. The increased water absorption is due to the presence of more hydroxyl and peptide groups in the CFF, which form hydrogen bonds. Additionally, water molecules can become trapped in the spaces within the composites, contributing to the higher water absorption rate.

4.3 Tensile Strength Analysis

The tensile test, performed according to ASTM-D-3039[43)], was carried out using a computerized universal testing machine (UTM). The environment was kept constant with regards to temperature, pressure, and relative humidity. The results of the tensile strength of the L-16 orthogonal array are presented in Table 8, and the main effect plots are displayed in Figure 6.

Table 8 Tensile Strength of Composite

Run Order	TiO_2 (%wt)	CFF (%wt)	ER (%wt)	Total (%Wt)	Tensile Strength (MPa)
1	0.50	2.15	97.36	100.00	49.84
2	0.50	4.85	94.67	100.00	54.21
3	0.50	5.93	93.60	100.00	56.38
4	0.50	7.58	91.96	100.00	58.61
5	1.00	2.15	96.87	100.00	53.74
6	1.00	4.85	94.20	100.00	57.18
7	1.00	5.93	93.13	100.00	61.84
8	1.00	7.58	91.50	100.00	64.31
9	1.50	2.15	96.38	100.00	55.14
10	1.50	4.85	93.72	100.00	57.38
11	1.50	5.93	92.66	100.00	60.87
12	1.50	7.58	91.04	100.00	64.37
13	2.00	2.15	95.89	100.00	60.23
14	2.00	4.85	93.24	100.00	62.71
15	2.00	5.93	92.19	100.00	64.35
16	2.00	7.58	90.57	100.00	66.12

Improving the interfacial adhesion that exists between the fiber and the matrix can lead to improvements in the material's mechanical characteristics like tensile strength etc. Through the use of chemical treatment, the surface of the fiber may be modified, resulting in an improvement in the interfacial adhesion[53]. In the current investigation, the CFF was mechanically characterized after undergoing chemical modification using a solution of 5 weight percent NaOH. The composites' mechanical characteristics can be improved by adding more nanoparticles, as was done[7, 8, 11, 12].

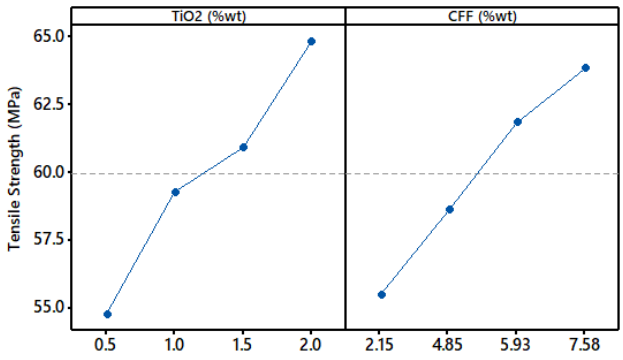

Figure 6 Tensile Strength (MPa) analysis for L-16 orthogonal array

The Microstructure images of the compsoite at highest tensile strength properties were present in Appendix A.

4.4 Wear Analysis

Evaluation of the sliding wear parameters of the composite material was carried out in line with the standard ASTM G-99-17[54]. After being polished and cleaned, the composite specimen was then forced up against a steel disc with an HRC-65 finish[1]. When conducting an analysis of sliding wear behavior on test specimens, the normal load was maintained in accordance with the orthogonal array, and the speed was likewise adjusted in accordance with the orthogonal array. Using the following equation, we were able to determine the particular wear rate shown by the composite specimen. The wear analysis was discuss as per signal to noise results which are list out in table 9, in which specific wear rate was calculated as per shown in equation 4.

$$Sp.Wear_{rate} = \frac{\Delta m}{\rho_{com}.speed.Time.F_{load}} \quad (4)$$

Table 9 Sp. Wear rate analysis of composite L-16 experiment table

Run Order	A	B	C	D	Sp. Wear Rate	S/N Ratio
1	0.5	1	1	200	2.08	-6.36
2	0.5	2	1.5	250	2.2	-6.85
3	0.5	3	2	300	2.89	-9.22
4	0.5	4	2.5	350	3.08	-9.77
5	1	1	1.5	300	2.31	-7.27
6	1	2	1	350	2.67	-8.53
7	1	3	2.5	200	1.87	-5.44
8	1	4	2	250	2.17	-6.73
9	1.5	1	2	350	2.17	-6.73
10	1.5	2	2.5	300	2.13	-6.57
11	1.5	3	1	250	1.49	-3.46
12	1.5	4	1.5	200	1.28	-2.14
13	2	1	2.5	250	1.43	-3.11
14	**2**	2	2	200	1.34	-2.54
15	**2**	3	1.5	350	1.43	-3.11
16	**2**	4	1	300	1.34	-2.54

A: Wt% of TiO2, **B**: CFF layers, **C**: Load, **E**: Rotation Speed

4.4.1 Effect of Controlling factors

The ratio of signal to noise provides evidence that demonstrates the effect of controlling elements such as TIO_2 weight percent, CFF, load, and speed. The control

parameters that have a significant impact on wear rate may be understood by analyzing the difference between the maximum and minimum means of SNR. When there is a larger disparity between the SNR means, the control element tends to become more important[55]. The effect that the various control factors have on the wear rate is outlined in Table 10. According to the ordering of the factors, the one that has the largest impact on the wear of composites is the weight percentage of the TiO_2 nano particle. CFF in composite has the least amount of impact on wear rate, whereas the rotation speed of the disk is the second most dominant characteristic.

Table 10 Sp. Wear rate analysis of composite L-16 experiment table

Level	A	B	C	D
1	-8.05	-5.867	-5.224	-4.121
2	-6.992	-6.122	-4.843	-5.037
3	-4.726	-5.306	-6.305	-6.4
4	-2.824	-5.297	-6.221	-7.034
Delta	5.225	0.825	1.462	2.913
Rank	**1**	**4**	**3**	**2**

A: Wt% of TiO_2, **B**: CFF layers, **C**: Load, **E**: Rotation Speed
The main effect plots for all controlling factors were present in fig.7 and fig.8.

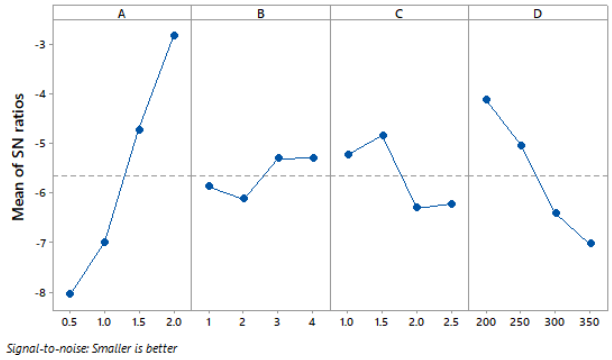

Figure 7 Signal to noise ratio analysis of sp. wear rate (Smaller is better)

When the rotational speed that is being applied is increased from 200 to 350 RPM, it is important to investigate that the rate of wear of composites also rises. The increase in speed causes the pin surface to become plastically distorted as a result of the high friction that is caused by the high level of contact between the surfaces. A high degree of plastic deformation can lead to the creation of subsurface cracks and an increased rate of material loss[1, 31, 54].

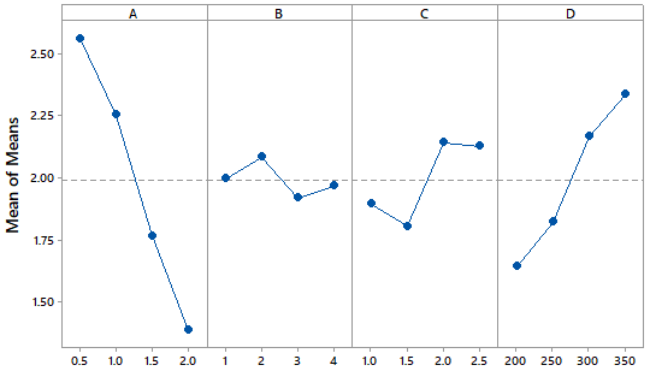

Figure 8 Mean analysis of sp. wear rate

The impact of the weight percentage of TiO_2 nanoparticles on the wear rate is demonstrated in the Main Effect Plots (MEPs) shown in Figures 7 and 8. An increase in the weight percentage of TiO_2 particles from 0.5 to 2.0 results in a decrease in the wear rate. This decrease in wear rate is attributed to the formation of a solid lubricant bond between the base particles and the nanoparticles. The load also has a mixed effect on the wear rate due to the mixing of CFF and nano particles in the base materials. Figure 7 and 8 show that the CFF has the least impact on the wear rate. The first two layers of CFF increase the wear rate, but more layers lead to a decrease in wear rate.

The data means that are close to the horizontal line suggest that the control variable had a much smaller impact on determining the wear rate. In contrast, a steeper line implies that the specific component has a stronger influence on the wear rate than the average. In this case, the steeper lines for Weight % of TiO_2 and Speed indicate that they are the key factors affecting the wear rate.

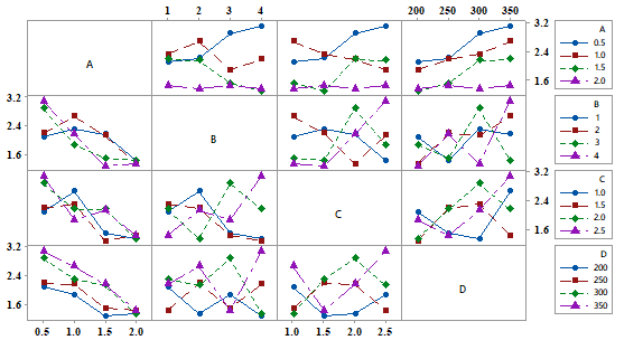

Figure 9 Interaction plots of sp. wear rate

Figure 9 shows the interaction graphs between the control variables and the cumulative effect of their individual impacts on the wear rate for the specimens. Optimal wear rate can be achieved by combining the control factors, such as a 2% weight of TiO2, 3 layers of CFF, 1.5 kilograms of load, and a rotating speed of 200 revolutions per minute.

4.4.2 Analysis of Variance (ANOVA) of Controlling factors

The results of the experiment were put via the ANOVA analysis tool so that they could be understood. An analysis of variance (ANOVA) was performed to determine the percentage impact of each control component (TiO_2 wt.%, CFF, Load and Rotation) on the wear rate displayed in Table 11.

Table 11 ANOVA table for control factors and Wear rate

Source	DF	SS	Contribution	MS	F-Value	P-Value	S/NS
Model	4	4.64031	93.93%	1.16008	42.57	0.0	S
Linear	4	4.64031	93.93%	1.16008	42.57	0.0	S
A	1	3.23208	65.43%	3.23208	118.59	0.0	S
B	1	0.01301	0.26%	0.01301	0.48	0.50	NS
C	1	0.21424	4.34%	0.21425	7.86	0.01	S
D	1	1.18098	23.91%	1.18098	43.33	0	S
Error	11	0.29979	6.07%	0.02725			
Total	15	4.9401	100.00%				

A: Wt% of TiO_2, B: CFF layers, C: Load, E: Rotation Speed, S: Significance, NS: Non Significance

The analysis of the variance was carried out with a degree of confidence of 95%, or a level of significance of 5%. If the P-value was less than 0.005, it suggested that the control parameter had a significant impact on the wear rate[56]. The results of the ANOVA table indicate that the TiO_2 nanoparticle, applied force, and rotation of the disk all have p-values below 0.005, making them highly influential factors in controlling the wear rate of the composite material. TiO_2 nanoparticle was found to be the most influential component, with a contribution of 65.43% to the wear rate. The rotation of the disk was the second most significant factor, contributing 23.91%. On the other hand, the load factor had a contribution of 4.34%, despite having the least impact on the wear rate. Overall, the TiO_2 nanoparticle and rotation were identified as the most relevant characteristics, while the CFF layers were found to be inconsequential.

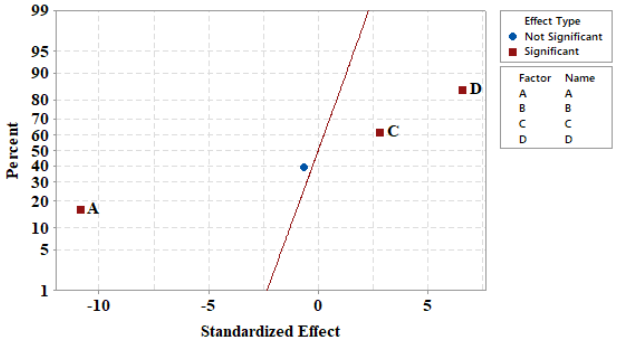

Figure 10 Normal plot to show the Significant factors for wear rate

4.4.3 Regression modeling of Sp. Wear Rate

A regression equation was built for the control components as well as the wear rate, and it is displayed below. The Normal plot and Pareto plot for the developed regression equation was shown in figure 10 and figure 11 respectively.

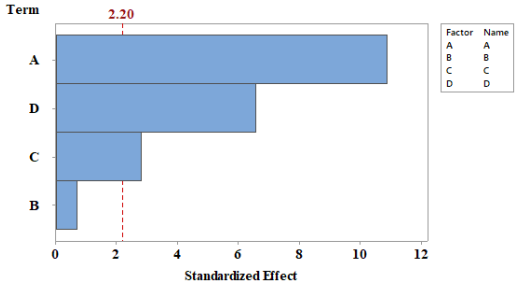

Figure 11 Pareto plot for the factors for wear rate

$$Wear\ Rate_{Sp.} = 1.36 - 0.8 * A(TiO_2) - 0.025 * B(CFF_{Layers}) + 0.21 * C(Load) + 0.0048 * D(Rotation_{Disk}) \ldots\ldots\ldots(5)$$

Figure 12 depicts the curve fitting that was done for the projected and original wear rate values, and table 12 displays the model summary.

Table 12 Model Summary for control factors and Wear rate regression equation

S	R-sq	PRESS
0.165087	93.93%	0.59614

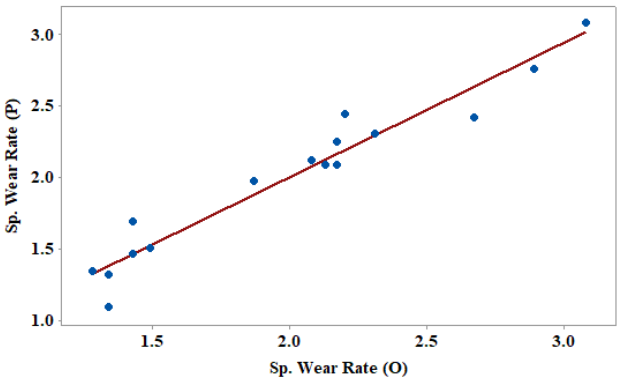

Figure 12 Curve fitting plot for the sp. wear rate

5. Conclusion

The utilization of the hand lay approach in the development of epoxy resin composites (ERC) incorporating TiO_2 nanoparticles and CFF layers resulted in highly successful outcomes. The hand lay approach, although challenging during fabrication, was used to create the composite and the experiment table was constructed using the Taguchi approach. The weight percentage of CFF and TiO_2 in the composite had a direct impact on its properties, with the weight percentage of TiO_2 having the most significant influence on the composite's wear rate.

An increase in the total weight percentage of CFF in the composite material led to a rise in the total weight percentage of void fraction. However, the presence of TiO_2 acted as a regulator, and when the matrix component epoxy resin was increased in relation to the nano particle size, the void fraction decreased. The mixing of CFF with epoxy resulted in an increase in the material's water absorption capacity, as CFF is hydrophilic and epoxy is hydrophobic. This increase was due to the formation of hydrogen bonds between the hydroxyl and peptide groups in CFF and the epoxy resin.

The weight percentage of TiO_2 nanoparticle was found to have the largest influence on the amount of wear experienced by the composite, with a contribution of 65.43% according to the results of the ANOVA table. The rotation speed of the disk was found to be the second most significant factor, with a contribution of 23.91%, while CFF in the composite had the least impact on the wear rate. In conclusion, the utilization of the hand lay approach and the incorporation of TiO_2 nanoparticles and CFF layers in the development of ERC composites showed promising results. The weight percentage of CFF and TiO_2 had a direct impact on the composite's properties, with TiO_2 having the most significant influence on the composite's wear rate. The findings of the ANOVA table reinforced this, showing the contribution of TiO_2 to be the largest at 65.43%, followed by rotation speed at 23.91% and CFF at 4.34%. The successful utilization of these components in the development of ERC composites has the potential to lead to further advancements in the field.

Graphical Abstract

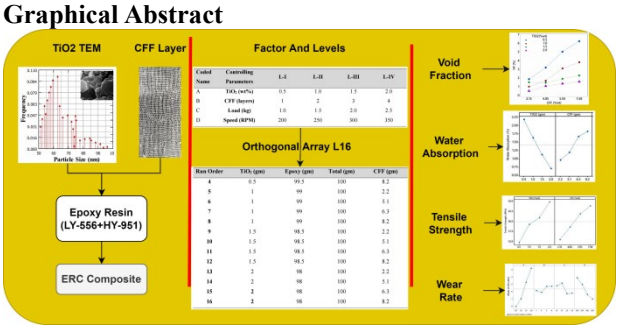

Appendix A: Fracture Images of the Composite (SEM)

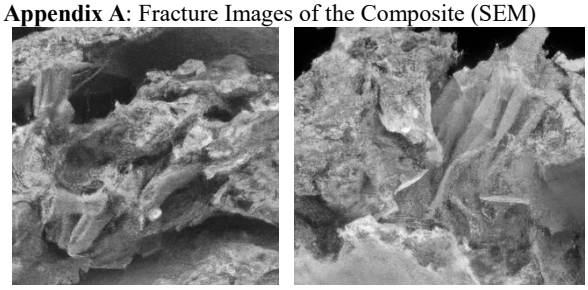

a.) Fracture of the Composite after UTM testing for highest CFF and Highest TiO_2 composite

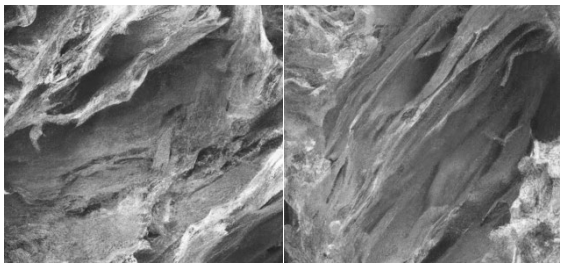

b.) Fracture of the Composite after UTM testing for Neat Composite made by Epoxy Resin Only

Figure 12 SEM images for hybrid and neat composite test object after fracture

References

1) Ranakoti, Lalit & Gangil, Brijesh & Rajesh, Pawan & Singh, Tej & Sharma, Shubham & Li, Chang & R.A., Ilyas & Mahmoud, Omar. (2022). Effect of surface treatment and fiber loading on the physical, mechanical, sliding wear, and morphological characteristics of tasar silk fiber waste-epoxy composites for multifaceted biomedical and engineering applications: Fabrication and characterizations. Journal of Materials Research and Technology. 19. 10.1016/j.jmrt.2022.06.024.
2) Jawaid M, Siengchin S. Hybrid composites: a versatile materials for future. Appl. Sci. Eng. Prog 2019;12(4). 223-223.
3) Ranakoti L, Gupta MK, Rakesh PK. Analysis of mechanical and tribological behavior of wood flour filled glass fiber reinforced epoxy composite. Mater Res Express 2019;6(8):085327.
4) Reddy BM, Mohana Reddy YV, Mohan Reddy BC, Reddy RM. Mechanical, morphological, and

thermogravimetric analysis of alkali-treated Cordia-Dichotoma natural fiber composites. J Nat Fibers 2020;17(5):759e68.

5) Chen S, Cheng L, Huang H, Zou F, Zhao HP. Fabrication and properties of poly (butylene succinate) biocomposites reinforced by waste silkworm silk fabric. Compos Appl Sci Manuf 2017;95:125e31.
6) Baghel, R, Chaturvedi, V, Pandel, B, & Pandel, U, "Utilization of Mining and Industrial Waste: A Sustainable Approach", Procedia Earth and Planetary Science, 11, 242–246. https://doi.org/10.1016/j.proeps, 2015
7) B. Suresha, S.L. Guggare, N.V. Raghavendra, Effect of TiO2 filler loading on physico-mechanical properties and abrasion of jute fabric reinforced epoxy composites, Mater. Sci. Appl. 7 (9) (2016) 510–526.
8) Siddhartha, V., Patnaik, A. and Bhatt, A.D. (2011) Mechanical and Dry Sliding Wear Characterization of Epoxy-TiO2 Particulate Filled Functionally Graded Composites Materials Using Taguchi Design of Experiment. Materials & Design, 32, 615-627. http://dx.doi.org/10.1016/j.matdes.2010.08.011
9) Li W, Qiao X, Sun K, Chen X. Mechanical and viscoelastic properties of novel silk fibroin fiber/poly (ε-caprolactone) biocomposites. J Appl Polym Sci 2008;110(1):134e9.
10) Ho MP, Lau KT, Wang H, Bhattacharyya D. Characteristics of a silk fibre reinforced biodegradable plastic. Compos B Eng 2011;42(2): 117e22.
11) P.A. Prasob, M. Sasikumar, Static and dynamic behavior of jute/epoxy composites with ZnO and TiO2 fillers at different temperature conditions, Polym. Test. 69 (2018) 52–62.
12) K. Kumar, P.K. Ghosh, A. Kumar, Improving mechanical and thermal properties of TiO2-epoxy nanocomposite, Compos. B Eng. 97 (2016) 353–360.
13) F.Z. Alshammari, K.H. Saleh, B.F. Yousif, A. Alajmi, A. Shalwan, J.G. Alotaibi, The influence of fibre orientation on tribological performance of jute fibre reinforced epoxy composites considering different mat orientations, Tribol. Ind. 40 (3) (2018) 335–348.
14) Bhargav, Middemeedi & Valasingam, Suresh. (2021). Experimental investigation of fiber orientation effect on mechanical and erosive wear performance of TiO2 filled woven jute fiber based epoxy composites. Materials Today: Proceedings. 44. 10.1016/j.matpr. 2020.12.660.
15) Suresha, B., Chandramohan, G., Praksah, J.N., Balu Samy, V. and Sankaranarayana Samy, V. (2006) The Role of Fillers on Friction and Slide Wear Characteristics in Glass-Epoxy Composite Systems. Journal of Minerals Materials Characterization and Engineering, 5 87-101. http://dx.doi.org/10.4236/jmmce.2006.51006
16) Moloney, A.C., Kausch, H.H., Kasier, T. and Beer, H.R. (1987) Parameters Determining the Strength and Toughness of Particulate Filled Epoxide Resins. Journal of Material Science, 22, 381-393. http://dx.doi.org/10.1007/bf01160743
17) Narkis, M., Nicolais, L. and Joseph, E. (1978) The Elastic Modulus of Particulate-Filled Polymers. Journal of Applied Polymer Science, 22, 2391-2394. http://dx.doi.org/10.1002/app.1978.070220829
18) Manson, J.A. and Sperling, L.H. (1976) Polymer Blends and Composites. Plenum Press, New York and London. http://dx.doi.org/10.1007/978-1-4615-1761-0
19) Osmani, A. (2009) Mechanical Properties of Glass-Fiber Reinforced Epoxy Composites Filled with Al2O3 Particles. Journal of Reinforced Plastics and Composites, 28, 2861-2867. http://dx.doi.org/10.1177/0731684408093975
20) Alavudeen, A., Rajini, N., Karthikeyan, S., Thiruchitrambalam, M. and Venkateshwaren, N. (2015) Mechanical Properties of Banana/Kenaf Fiber-Reinforced Hybrid Polyester Composites: Effect of Woven Fabric and Random Orientation. Materials & Design, 66, 246-257. http://dx.doi.org/10.1016/ j.matdes.2014.10.067
21) Swain, P.T.R. and Biswas, S. (2014) Physical and Mechanical Behavior of Al2O3 Filled Jute Fiber Reinforced Epoxy Composites. International Journal of Current Engineering & Technology, 2, 67-71. http://dx.doi.org/10.14741/ijcet/spl.2.2014.13
22) Mantry, S., Satapathy, A., Jha, A.K., Singh, S.K. and Patnaik, A. (2011) Preparation, Characterization and Erosion Response of Jute-Epoxy Composites Reinforced with Sic Derived from Rice Husk. International Journal of Plastics and Technology, 15, 69-76. http://dx.doi.org/10.1007/s12588-011-9007-z
23) Wu, L., Guo, X. and Zhang, J. (2014) Abrasive Resistant Coatings—A Review. Lubricants, 2, 66-89. http://dx.doi.org/10.3390/lubricants2020066
24) El-Tayeb, N.S.M. (2008) A Study on the Potential of Sugarcane Fibers/Polyester Composite for Tribological Applications. Wear, 265, 223-235. http://dx.doi.org/10.1016/j.wear.2007.10.006
25) Yousif, B.F. and El-Tayeb, N.S.M. (2007) Effect of Oil Palm Fibres as Reinforcement on Tribological Performance of Polyester Composite. Surface Review and Letters, 14, 1095- 1102. http://dx.doi.org/10.1142/S0218625X07010561
26) Raadnui, S. (2006) The Abrasive Wear Behaviour of a Thai-Silk Fabric. International Journal of Applied Mechanics and Engineering, 11, 755-763. http://www.ijame.uz.zgora.pl/ijame_files/archives/v11PDF/n4/755-763_Article_04.pdf
27) Tong, J., Ma, Y., Chen, D., Sun, J. and Ren, L. (2005) Effects of Vascular Fiber Content on Abrasive Wear of Bamboo. Wear, 259, 78-83. http://dx.doi.org/10.1016/j.wear.2005.03.031
28) Chand, N., Dwivedi, U.K. and Acharya, S.K. (2007) Anisotropic Abrasive Wear Behaviour of Bamboo

(Dentrocalamus strictus). Wear, 262, 1031-1037. http://dx.doi.org/10.1016/j.wear.2006.10.006
29) Khan, M.A., Ahmed Joshi, S. and Al Said, S.A.F. (2014) Abrasive Wear Behaviour of Chemically Treated Coir Fibre Filled Epoxy Polymer Composites. American Journal of Mechanical Engineering and Automation, 1, 1-5. http://www.openscienceonline.com/journal/ajmea
30) Basumatary, K.K., Mohanta, N. and Acharya, S.K. (2014) Effect of Fiber Loading on Abrasive Wear Behaviour of Ipomoea Carnea Reinforced Epoxy Composite. International Journal of Plastic Technology, 18, 64-74. http://dx.doi.org/10.1007/s12588-014-9065-0
31) Divya, G.S., Ananad, K. and Suresha, B. (2014) Wear Behaviour of Coir Reinforced Treated and Untreated Hybrid Composites. International Journal of Innovative Research and Development, 4, 632-639. www.ijird.com
32) Siva, I., Winowlin Jappes, J.T. and Suresha, B. (2012) Investigation on Mechanical and Tribological Behaviour of Naturally Woven Coconut Sheath-Reinforced Polymer Composites. Polymer Composites, 33, 723-732. http://dx.doi.org/10.1002/pc.22197
33) Thirumalai R, Prakash R, Ragunath R, SenthilKumar KM. Experimental investigation of mechanical properties of epoxy based composites. Mater Res Express 2019;6(7):075309.
34) Mittal V, Saini R, Sinha S. Natural fiber-mediated epoxy compositesea review. Compos B Eng 2016;99: 425e35.
35) Karthik, K., Rajamani, D., Raja, T., & Subramani, K. (2022). Experimental investigation on the mechanical properties of Carbon/Kevlar fibre reinforced epoxy LY556 composites. Materials Today: Proceedings, 52, 668-674.
36) Yashas Gowda, T. G., Vinod, A., Madhu, P., Sanjay, M. R., Siengchin, S., Jawaid, M., Polym. Compos. 2022, 1. https://doi.org/10.1002/pc.26814
37) Sivasaravanan, S., & Raja, V. B. (2014). Impact characterization of epoxy LY556/E-glass fibre/nano clay hybrid nano composite materials. Procedia Engineering, 97, 968-974.
38) Rangi A, Jajpura L. The biopolymer sericin: extraction and applications. J Text Sci Eng 2015;5(1): 1e5.
39) Gallart-Ayala H, Moyano E, Galceran MT. Fast liquid chromatographyetandem mass spectrometry for the analysis of bisphenol A-diglycidyl ether, bisphenol Fdiglycidyl ether and their derivatives in canned food and beverages. J Chromatogr A 2011;1218(12): 1603e10.
40) Egala, Rajesh; Gangi Setti, Srinivasu (2018). Impact characterization of epoxy LY556/ricinus communis L plant natural fiber composite materials. Materials Today: Proceedings, 5(13), 26799–26803. doi:10.1016/j.matpr.2018.08.159
41) Rueden, C.T., Schindelin, J., Hiner, M.C. et al. ImageJ2: ImageJ for the next generation of scientific image data. BMC Bioinformatics 18, 529 (2017). https://doi.org/10.1186/s12859-017-1934-z
42) Kuppusamy, R. R. P., Rout, S., & Kumar, K. (2020). Advanced manufacturing techniques for composite structures used in aerospace industries. Modern Manufacturing Processes, 3–12. https://doi.org/10.1016/B978-0-12-819496-6.00001-4
43) Miller A, Brown C, Warner G. Guidance on the use of existing ASTM polymer testing standards for ABS parts fabricated using FFF. Smart Sustain. Manuf. Syst 2019;3(1).
44) Deshpande S, Rangaswamy T. Effect of fillers on E-glass/jute fiber reinforced epoxy composites. Int J Eng Res 2014;4(8):118e23.
45) Zhang P, Bao J, Jiang Z, Dong B, Chen X. Enhancing thermooxidative stability of thermoset polyimide composites using nano neodymium oxide particles. J Mater Res Technol 2021;14:2638e49.
46) Gholampour A, Ozbakkaloglu T. A review of natural fiber composites: properties, modification and processing techniques, characterization, applications. J Mater Sci 2020;55(3):829e92.
47) Minitab 17 Statistical Software (2010). [Computer software]. State College, PA: Minitab, Inc. (www.minitab.com)
48) Sathish T, Karthick S. Wear behaviour analysis on aluminium alloy 7050 with reinforced SiC through taguchi approach. J Mater Res Technol 2020;9(3): 3481e7.
49) Yong L, Jian L, Xian L, Bei W. Test and analysis of the porosity of cotton fiber assembly. Journal of Engineered Fibers and Fabrics. January 2021. doi:10.1177/15589250211024225
50) Abbott, AM, Higgerson, GJ, Long, RL, et al. An instrument for determining the average fiber linear density (fineness) of cotton lint samples. Text Res J 2010; 80: 1–12.
51) Dadhich, Manish & Prajapati, Om & Sharma, Vikas. (2021). Investigation of boiling heat transfer of titania nanofluid flowing through horizontal tube and optimization of results utilizing the desirability function approach. Powder Technology. 378. 104-123. 10.1016/j.powtec.2020.09.077.
52) Panda N, Biswas A, Sukla LB, Pramanik K. Degradation mechanism and control of blended eri and tasar silk nanofifiber. Applied biochemistry and biotechnology 2014;174(7):2403e12.
53) Bozaci E, Sever K, Sarikanat M, Seki Y, Demir A, Ozdogan E, et al. Effects of the atmospheric plasma treatments on surface and mechanical properties of flflax fifiber and adhesion between fifiberematrix for composite materials. Compos B Eng 2013;45(1): 565e72.
54) Raju P, Raja K, Lingadurai K, Maridurai T, Prasanna

SC. Mechanical, wear, and drop load impact behavior of glass/ Caryota urens hybridized fifiber-reinforced nanoclay/SiC toughened epoxy multihybrid composite. Polym Compos 2021;42(3):1486e96.

55) Veličković S, Stojanović B, Babić M, Bobić I. Optimization of tribological properties of aluminum hybrid composites using Taguchi design. Journal of Composite Materials. 2017;51(17):2505-2515. doi:10.1177/0021998316672294
56) Bhuvanesh D, Radhika N, Vidyapeetham AV. Experimental investigation on tribological characteristics of silicon nitride reinforced aluminium metal matrix composites. J Eng Sci Technol 2017;12 (5):1295e306.
57) A. Mahyudin, S. Arief, H.Abral, M. Muldarisnu, M.P. Artika, "Mechanical Properties and Biodegradability of Areca Nut Fiber-reinforced Polymer Blend Composites," Evergreen, 7(3), 366-372 (2020).
58) H. Sosiati, Y.A. Shofie, A.W. Nugroho, "Tensile properties of Kenaf/E-glass reinforced hybrid polypropylene (PP) composites with different fiber loading,"Evergreen, 5 (2), 1-5 (2018).
59) A. Kumar, A.K. Chanda, S. Angra, "Optimization of Stiffness Properties of Composite Sandwich using Hybrid Taguchi-GRA-PCA,"Evergreen, 8 (2), 310-317 (2021).
60) H Fayaz, K Karthik, KG Christiyan, M Arun Kumar, A Sivakumar, S Kaliappan, M Mohamed, Ram Subbiah, Simon Yishak, (2022), An Investigation on the Activation Energy and Thermal Degradation of Biocomposites of Jute/Bagasse/Coir/Nano TiO2/ Epoxy-Reinforced Polyaramid Fibers, Journal of Nanomaterials, Journal of Nanomaterials, Hindawi, Volume2022, ArticleID 3758212, pages5 https://doi. org/10.1155/2022/3758212.
61) Karthik, K., Rathinasuriyan, C., Raja, T. and Sankar, R., 2022. Mechanical Characterization of Kenaf/Carbon Fiber Reinforced Polymer Matrix Composites with Different Stacking Sequence. In Bio-Fiber Reinforced Composite Materials (pp. 175-187). Springer,
62) Krishnasamy Karthik, Jayavelu Udaya Prakash, Joseph Selvi Binoj, Bright Brailson Mansingh,(2022), Effect of stacking sequence and silicon carbide nanoparticles on properties of carbon/glass/Kevlar fiber reinforced hybrid polymer composites, polymer composites, Volume 43, Issue 9, .Pages 6096–6105..https://doi.org/10.1002/pc.26912.
63) Karthik, K., Rajamani, D., Manimaran, A., Udaya Prakash, J.(2020), Wear behaviour of hybrid polymer matrix composites using Taguchi technique, Materials Today: Proceedings, 2020, 33, pp. 3186–3190.
64) Karthik, K., Manimaran, A., Veerendra Rayudu, J., Sharma, D.(2017), Optimization of the process parameter in drilling of GFRP using HSS drill, International Journal of Mechanical and Production Engineering Research and Development, 7(6), pp. 403–408.
65) Xiong, S., Liang, D., Wu, H., Lin, W., Chen, J., & Zhang, B. (2021). Preparation, characterization, tribological and lubrication performances of Eu doped CaWO4 nanoparticle as anti-wear additive in water-soluble fluid for steel strip during hot rolling. Applied Surface Science, 539, 148090.
66) Xiong, S., Zhang, X. & Liang, D. Preparation, microstructure and luminescence properties of TiO2/WO3 composites. Appl. Phys. A 128, 778 (2022).https://doi.org/10.1007/s00339-022-05920-3
67) XIONG S, ZHANG B, LUO S, et al. Preparation, characterization, and tribological properties of silica-nanoparticle-reinforced B-N-co-doped reduced graphene oxide as a multifunctional additive for enhanced lubrication. Friction, 2021, 9(2):239-249. https://doi.org/10.1007/s40544-019-0331-1